Direct Synthesis of Highly Crystalline and Monodisperse Manganese Ferrite Nanocrystals

Eunae Kang,[†] Jongnam Park,[†] Yosun Hwang,[‡] Misun Kang,[‡] Je-Geun Park,[‡,§] and Taeghwan Hyeon*,[†]

National Creative Research Initiative Center for Oxide Nanocrystalline Materials and School of Chemical Engineering, Seoul National University, Seoul 151-744, Korea, Department of Physics, Sungkyunkwan University, Suwon 440-746, Korea, and Center for Strongly Correlated Materials Research, Seoul National University, Seoul 151-742, Korea

Received: March 3, 2004; In Final Form: June 16, 2004

Highly crystalline and monodisperse manganese ferrite nanocrystals were synthesized via the thermal decomposition of metal-surfactant complexes followed by mild chemical oxidation. Particle sizes could be varied from 5 to 13 nm by changing the experimental parameters. The uniformity of the nanocrystals was demonstrated by the formation of two- and three-dimensional superlattices. Electron diffraction, X-ray diffraction, and high-resolution TEM images confirmed the high crystallinity of the manganese ferrite nanocrystals. Elemental analysis and energy-dispersive X-ray spectroscopy confirmed that the molar ratio of Mn:Fe was 1:2. The nanocrystals were found to exhibit the typical behaviors of magnetic nanocrystals with the characteristic narrow energy barrier distributions of magnetic anisotropy, confirming the uniformity of the nanocrystals.

The synthesis of uniformly sized magnetic nanoparticles has been intensively pursued because of their broad applications including magnetic storage media, ferrofluids, magnetic resonance imaging (MRI), magnetically guided drug delivery, and catalysts for the growth of carbon nanotubes.[1,2] Several metallic magnetic nanocrystals have been synthesized via thermal decomposition of organometallic precursors or reduction of metal salts.[3] Many ferrite nanoparticles have been synthesized using reverse micelles as nanoreactors.[4] Thermal decomposition of precursors has been also used to synthesize ferrite nanoparticles.[5] However, an exhaustive size selection process was usually required to obtain magnetic nanocrystals with a uniform particle size distribution. Recently, several groups reported the direct synthesis of monodisperse ferrite nanocrystals without a size-selection process. Our group reported the direct synthesis of highly crystalline and monodisperse ferrite nanocrystals via the thermal decomposition of metal-surfactant complexes followed by mild chemical oxidation.[6] Similarly, Sun and coworkers produced monodisperse ferrite nanocrystals via a high-temperature solution phase reaction of metal acetylacetonate with 1,2-hexadecanediol in the presence of surfactants.[7] Herein we report on the synthesis of monodisperse and highly crystalline manganese ferrite ($MnFe_2O_4$) nanocrystals with particle sizes ranging from 5 to 13 nm.

The synthetic procedure reported here is the modified version of a method that was used by our group for the synthesis of monodisperse nanocrystals of metal oxides and metal sulfides, which employs the formation of a metal-surfactant complexes followed by aging at high temperature.[1a,6,8] Iron pentacarbonyl ($Fe(CO)_5$) and dimanganese decacarbonyl ($Mn_2(CO)_{10}$) were used as the metal precursors. First, iron−manganese alloy nanoparticles were formed by the thermal decomposition of Fe−Mn-oleate complex, which was generated from the reaction of Iron pentacarbonyl and dimanganese decacarbonyl in the presence of oleic acid. The resulting alloy nanoparticles were oxidized using trimethylamine *N*-oxide to obtain manganese ferrite nanocrystals. The following procedure describes a typical synthesis of 10 nm sized manganese ferrite nanocrystals. 0.175 g of $Mn_2(CO)_{10}$ (0.45 mmol) was mixed with 10 g of octyl ether and 2.3 mL of oleic acid (7.26 mmol) at room temperature under an argon atmosphere. The resulting mixture was slowly heated to 130 °C with intermittent shaking to prevent the sublimation of $Mn_2(CO)_{10}$. When the solution temperature reached 130 °C, 0.2 mL of $Fe(CO)_5$ (1.52 mmol) was rapidly added to the mixture, and then the resulting solution was heated to reflux (∼300 °C) and kept at this temperature for 1 h. The color of the reaction mixture changed from an initial yellow color to colorless at 250 °C, and finally to black at the reflux temperature. The disappearance of the solution color at 250 °C demonstrated the formation of a kind of Fe−Mn-oleate complex, which was too air-sensitive to characterize. The black solution was cooled to room temperature, and then 0.34 g of dehydrated trimethylamine *N*-oxide (4.53 mmol) was added to the solution. Afterward, the solution was then heated to 140 °C under an argon atmosphere and kept at this temperature for 1 h, before being further heated to reflux and maintained at this temperature for 1 h. The solution was finally cooled to room temperature and 100 mL of ethanol was added to yield a black precipitate. The final nanocrystals were obtained in a powder form by centrifugation. The powdery nanocrystals were found to be readily dispersable in many organic solvents including hexane, toluene, and chloroform.

We attempted the thermal decomposition of the Mn-oleate complex, which was generated from the reaction of dimanganese decacarbonyl with oleic acid in octyl ether, to synthesize manganese nanoparticles. However, the Mn-oleate complex was not decomposed and no manganese nanoparticles were produced

* To whom correspondence should be addressed. E-mail: thyeon@plaza.snu.ac.kr.
[†] School of Chemical Engineering, Seoul National University.
[‡] Department of Physics, Sungkyunkwan University.
[§] Center for Strongly Correlated Materials Research, Seoul National University.

10.1021/jp049041y CCC: $27.50
Published on Web 08/19/2004

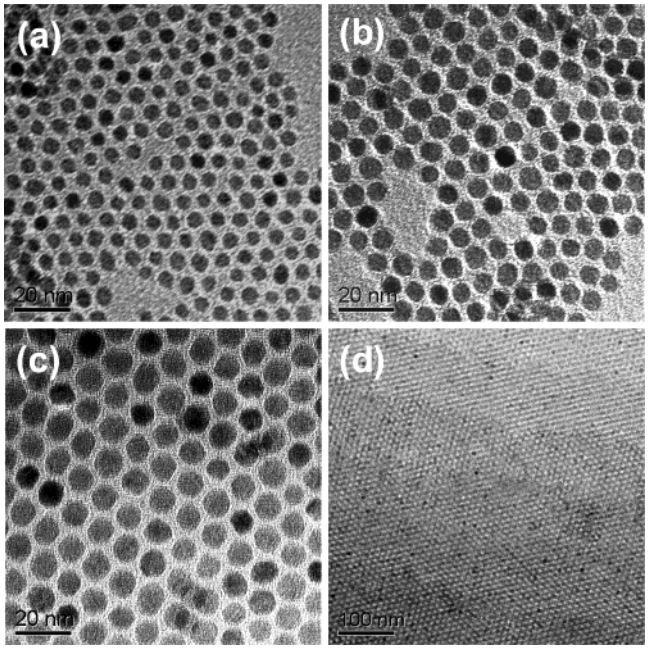

Figure 1. TEM image of manganese ferrite nanocrystals with particle sizes of (a) 5 nm, (b) 7 nm, and (c) 10 nm. (d) TEM image of 3-dimensional superlattice of 7 nm manganese ferrite nanocrystals. TEM images were obtained using a JEOL EM-2000 EX II microscope.

under these conditions. Interestingly enough, when $Fe(CO)_5$ was added to the Mn-oleate complex solution and the resulting mixture was refluxed, black colored nanoparticles were synthesized, as described above. The results demonstrate that Fe−Mn-oleate complexes were generated from the reaction of $Fe(CO)_5$ and $Mn_2(CO)_{10}$ with oleic acid and that these complexes were decomposed to produce Fe−Mn alloy nanoparticles.

The synthesized nanocrystals were characterized by low- and high-resolution transmission electron microscopy (TEM), X-ray diffraction (XRD), and energy-dispersive X-ray spectroscopy (EDX). Low- and high-resolution TEM images were obtained using a JEOL EM-2000 EX II microscope. XRD patterns were obtained with a Rigaku D/Max-3C diffractometer equipped with a rotation anode and a Cu Kα radiation source ($\lambda = 0.15418$ nm). The size uniformity of the nanocrystals was demonstrated by means of the TEM images shown in Figure 1. The TEM images showed that the nanocrystals are very uniform in size and that the diameters of the nanocrystals vary from 5 to 10 nm by changing the ratio of oleic acid to metal precursors. When starting reaction mixtures containing 1:1, 1:2, and 1:3 molar ratios of the metal precursors to oleic acid were used in the synthesis, manganese ferrite nanocrystals with particle sizes of 5, 7, and 10 nm were obtained, respectively. In some TEM images, well-aligned 3-dimensional superlattices were also observed, as shown in Figure 1d, demonstrating the uniformity of the nanocrystals. A further increase in the proportion of oleic acid did not result in the production of nanocrystals with larger particle-sizes. Instead, nanocrystals with a broad particle size distribution were obtained. Very similar results were observed in our previous synthesis of iron oxide nanocrystals.[6]

The XRD pattern of the 10 nm sized nanocrystals, shown in Figure 2, revealed that the nanocrystals had a *Fd*3*m* cubic spinel structure of manganese ferrite (JCPDS PDF# 10-0319). Because different bimetallic ferrite materials show similar XRD patterns, we carefully compared the observed peaks for the 10 nm sized nanocrystals with the known characteristic peaks in the XRD patterns of iron ferrite and manganese ferrite. The characteristic XRD peaks at 73.58°, 88.46°, and 103.66° confirmed that these

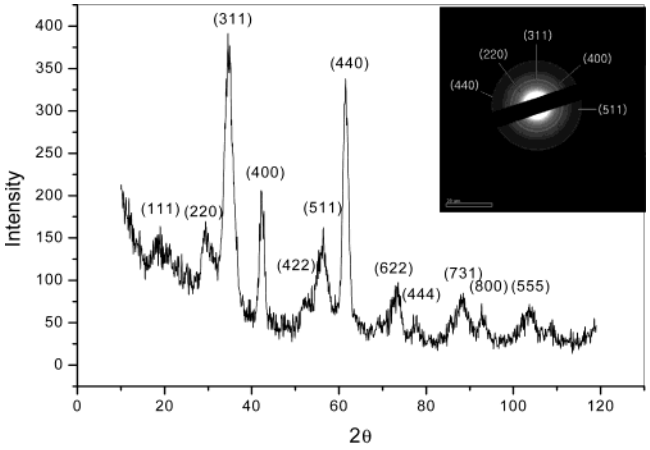

Figure 2. X-ray diffraction pattern of 10 nm manganese ferrite nanocrystals. The XRD pattern was obtained with a Rigaku D/Max-3C diffractometer equipped with a rotating anode and a Cu Kα radiation source ($\lambda = 0.154056$ nm). Inset is ED pattern obtained using a JEOL EM-2000 EX II microscope.

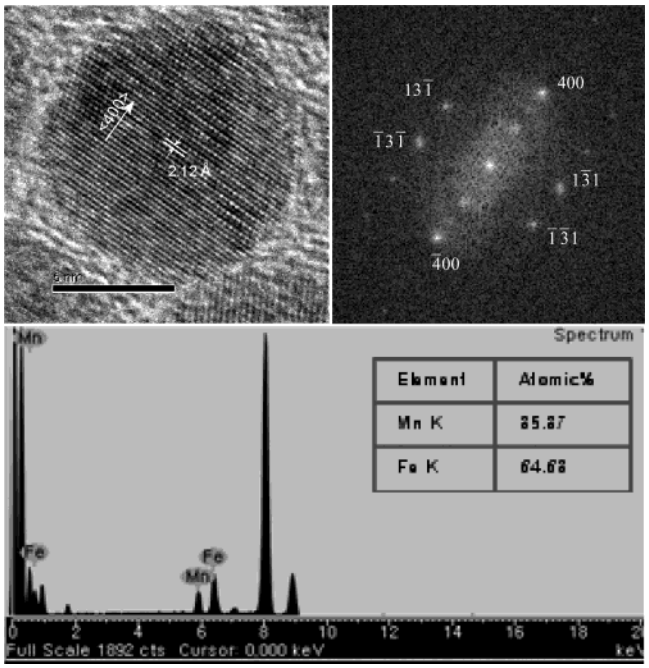

Figure 3. (a) High-resolution TEM image (top left), (b) FFT pattern (top right), and (c) EDX data (bottom) of 10 nm manganese ferrite nanocrystals.

nanocrystals were indeed manganese ferrite. The mean size of the nanocrystals calculated using the Scherrer formula was similar to that obtained by TEM. The structural properties of a 10 nm sized single nanocrystal were characterized using the high-resolution transmission electron micrograph (HRTEM). A HRTEM image of 10 nm sized nanocystal, shown in Figure 3a, illustrates the highly crystalline nature of the nanocrystals. The interplanar distance is estimated to be 2.12 Å, which is in good agreement with the {400} planes of the manganese ferrite. Figure 3b shows the fast Fourier transformation (FFT) pattern shown in Figure 3a, demonstrating that the nanocrystals have (400), ($1\bar{3}1$), and ($\bar{1}3\bar{1}$) planes with a zone axis of [013]. The elemental analysis using inductively coupled plasma atomic emission spectrometry (ICP-AES) confirmed the 1:2 molar ratio of Mn to Fe. The nanoscale elemental analysis using a energy-dispersive X-ray spectroscopy (EDX), shown in Figure 3c, also confirmed the Mn:Fe stoichiometry of 1:2, demonstrating the formation of $MnFe_2O_4$ nanocrystals. The composition of

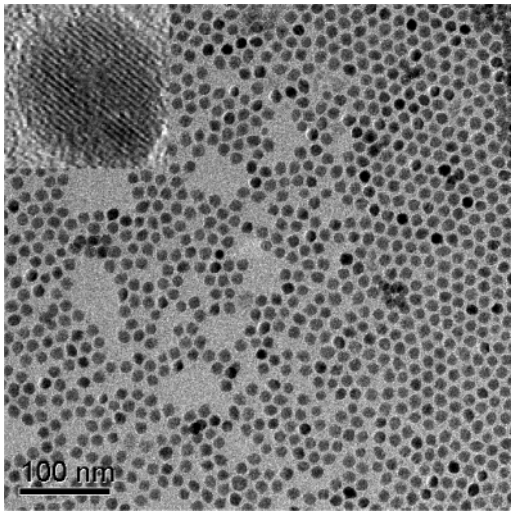

Figure 4. Low-resolution and High-resolution TEM images (inset) of 13 nm sized manganese ferrite nanocrystal with molar Fe:Mn ratio of 1.7:1. TEM images were obtained using a JEOL EM-2000 EX II microscope.

manganese ferrite could easily be controlled by varying the ratio of iron to manganese in the metal precursors, because the molar ratio of the final nanocrystals was invariably almost the same as that of the initially supplied iron and manganese precursors. As the relative amount of the manganese precursor increased, larger sized nanocrystals were produced. For example, when a precursor mixture with a Mn:Fe molar ratio of 1:1.5 was employed in the synthesis, we obtained manganese ferrite nanocrystals with a particle size of 13 nm and Mn:Fe stoichiometry of 1:1.7 (Figure 4).

Magnetic studies were carried out on 5, 7, and 10 nm sized powdery manganese ferrite nanocrystals, using a commercial vibrating sample magnetometer (Lake Shore 9300). The zero field cooling and field cooling (ZFC−FC) procedures were carried out from 2 to 350 K in an applied magnetic field of 100 Oe, to measure the temperature dependence of magnetization. Figure 5 shows the magnetization-temperature (MT) curves of typical nanocrystals. We normalized the magnetization in a conventional way of using the measured sample mass so the absolute value of the magnetization is likely to vary depending on the total amount of surfactant present inside the sample. With increasing temperatures, the ZFC magnetization data for each manganese ferrite nanocrystals increases before reaching a maximum value, i.e., the blocking temperature (T_B). At temperatures above T_B, the thermal energy, characterized by K_BT, is larger than the magnetic energy barrier, and, thus the materials become superparamagnetic following the Curie−Weiss law. The blocking temperatures of the 5, 7, and 10 nm sized manganese ferrite nanocrystals was found to be approximately 30, 60, and 85 K, respectively. These blocking temperatures correspond to magnetic anisotropy energies ranging from 9×10^5 to 4×10^5 erg/cm^3. These magnetic anisotropy energies are much larger than the bulk magnetic anisotropy energy of 2.5×10^4 erg/cm^3 at 100 K.[9] This increased magnetic anisotropy energy could be due to interparticle interactions because of the powder nature of our samples. To check if there exists such an effect of interparticle interactions on the magnetic anisotropy energy, we have measured the temperature dependence of the magnetization after ZFC as shown in Figure 5 as filled data points. For these measurements, we diluted the original powder samples using *p*-xylene to have about the same interparticle distance of 550 nm. As the signal of the diluted samples is very small for a vibrating sample magnetometer, we used an MPMS 5XL

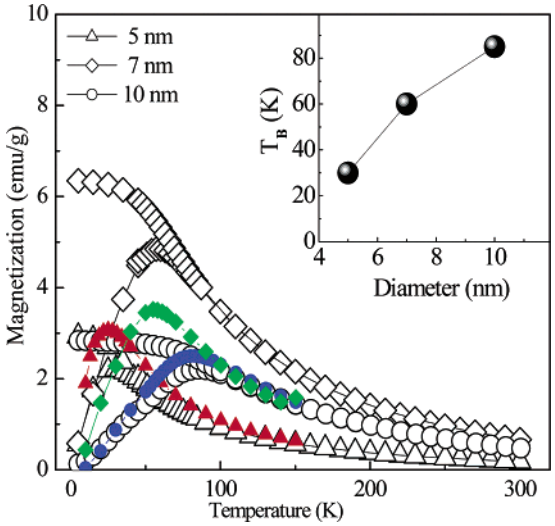

Figure 5. Zero-field cooled and field-cooled magnetization data measured in an applied field of 100 Oe of 5 nm (triangles), 7 nm (diamonds), and 10 nm (circles) manganese ferrite nanocrystals, respectively. The data shown as filled symbols were obtained from diluted samples after zero-field cooling: 5 nm (triangles), 7 nm (diamonds), and 10 nm (circles). Inset shows how blocking temperature T_B evolves with varying the diameters of nanocrystals.

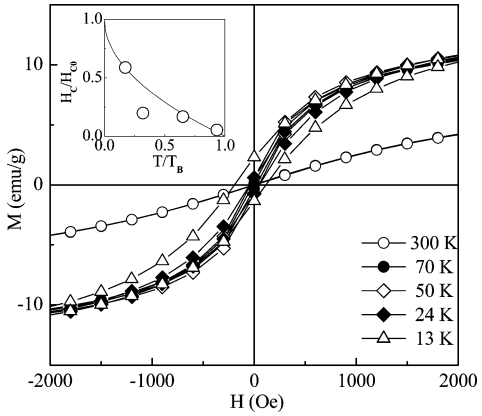

Figure 6. Magnetization vs applied magnetic field and temperature dependence of the coercive field (inset) for the $MnFe_2O_4$ nanocrystals with a diameter of 7 nm.

Quantum Design SQUID magnetometer for these measurements. As shown in Figure 5, these diluted samples show the temperature dependence that is similar to those of the powder samples and the blocking temperature drops only by ~5 K for all three diluted samples compared with the powder samples. This experimental observation then suggests that the increased magnetic anisotropy energy of our powder samples should be of intrinsic sample property, not due to the interparticle interactions. For higher magnetic fields, the blocking temperature moves toward lower temperature with roughly inversely proportional to the magnetic field. The field dependence of the magnetization for the 7 nm sized sample, shown in Figure 6, begins to exhibit field hysteresis with a coercive field of 150 Oe at 13 K. With increasing temperatures, the magnetic hysteresis becomes weaker and eventually disappears above the blocking temperature. This temperature dependence of the coercive field follows approximately the theoretical predictions for a single magnetic domain; $Hc/Hc_0 = 1 - (T/T_B)^{1/2}$, where Hc is the measured coercive field, Hc_0 the estimated coercive field at $T = 0$ K, T_B the measured blocking temperature. This observation reinforces our view that all our samples are in the single domain region. Similar magnetic properties were previ-

ously reported for $MnFe_2O_4$ nanocrystals synthesized via water-in-toluene reverse micelles.[10]

In conclusion, highly crystalline and monodisperse manganese ferrite nanocrystals were successfully synthesized via the thermal decomposition of metal-surfactant complexes, followed by mild oxidation using trimethylamine *N*-oxide. The synthetic procedure reported here has several important advantageous features over other conventional methods. First of all, well-separated spherical and monodisperse nanocrystals were obtained without having resort to a further size-selection process. Second, a simple mixture of iron pentacarbonyl and dimanganese decacarbonyl was employed as the precursors instead of the single molecular precursor which is very difficult to synthesize. Third, both the particle size and composition of the ferrite nanocrystals can be reproducibly controlled by varying the experimental conditions.

Acknowledgment. The work was supported by the National Creative Research Initiative Program of the Korean Ministry of Science and Technology. J.G.P. acknowledges Center for Strongly Correlated Materials Research, Seoul National University, for financial support.

References and Notes

(1) (a) Hyeon, T. *Chem. Commun.* **2003**, 927. (b) Fendler, J. H. *Nanoparticles and Nanostructured Films*; Wiley-VCH: Weinheim, Germany, 1998. (c) Schmid, G. *Nanoparticles: From Theory to Application*; Wiley-VCH: Weinheim, Germany, 2004. (d) Klabunde, K. J. *Nanoscale Materials in Chemistry*; Wiley-Interscience: New York, 2001. (e) Sun, S.; Murray, C. B.; Weller, D.; Folks, L.; Moser, A. *Science* **2000**, *287*, 1989. (f) Fertman, V. E. *Magnetic Fluids Guidebook: Properties and Applications*; Hemisphere Publishing Co.: New York, 1990. (g) Berkovsky, B. M.; Medvedev, V. F.; Krakov, M. S. *Magnetic Fluids: Engineering Applications*; Oxford University Press: Oxford, U.K., 1993. (h) O'Handley, R. C. *Modern Magnetic Materials*; Wiley: New York, 1999.

(2) (a) Awschalom, D. D.; DiVicenzo, D. P. *Phys. Today* **1995**, *4*, 43. (b) Leslie-Pelecky, D. L.; Rieke, R. D. *Chem. Mater.* **1996**, *8*, 1770. (c) Josephson, L.; Perez, J. M.; Weissleder, R. *Angew. Chem., Int. Ed.* **2001**, *40*, 3204. (d) Raj, K.; Moskowitz, R. *J. Magn. Magn. Mater.* **1990**, *85*, 233. (e) Speliotis, D. E. *J. Magn. Magn. Mater.* **1999**, *193*, 29. (f) Raj, K.; Moskowitz, B.; Casciari, R. *J. Magn. Magn. Mater.* **1995**, *149*, 174. (g) Oswald, P.; Clement, O.; Chambon, C.; Schouman-Claeys, E.; Frija, G. *Magn. Reson. Imaging* **1997**, *15*, 1025. (h) Hergt, R.; Andra, W.; d'Ambly, C. G.; Hilger, I.; Kaiser, W. A.; Richter, U.; Schmidt, H.-G. *IEEE Trans. Magn.* **1998**, *34*, 3745. (i) Jordan, A.; Scholz, R.; Wust, P.; Fähling, H.; Felix, R. *J. Magn. Magn. Mater.* **1999**, *201*, 413. (j) Kim, D. K.; Zhang, Y.; Kehr, J.; Klason, T.; Bjelke, B.; Muhammed. M. *J. Magn. Magn. Mater.* **2001**, *225*, 256. (k) Pankhurst, Q. A.; Connolly, J.; Jones, S. K.; Dobson, J. *J. Phys. D: Appl. Phys.* **2003**, *36*, R167. (l) Tartaj, P.; Morales, M. P.; Veintemillas-Verdaguer, S.; González-Carrenõ, T.; Serna, C. J. *J. Phys. D: Appl. Phys.* **2003**, *36*, R182. (m) Berry, C. C.; Curtis, A. S. G. *J. Phys. D: Appl. Phys.* **2003**, *36*, R198. (n) Dai, H. *Acc. Chem. Res.* **2002**, *35*, 1035. (o) Cheung, C. L.; Kurtz, A.; Park, H.; Lieber, C. M. *J. Phys. Chem. B* **2002**, *106*, 2429. (p) Tiefenauer, L. X.; Tscgirky, A.; Kuhne, G.; Andres, R. Y. *Magn. Reson. Imaging* **1996**, *14*, 391. (q) Högemann, D.; Josephson, L.; Weissleder, R.; Basilion, J. P. *Bioconjugate Chem.* **2000**, *11*, 941.

(3) (a) Park, S.-J.; Kim, S.; Lee, S.; Khim, Z. G.; Char, K.; Hyeon, T. *J. Am. Chem. Soc.* **2000**, *122*, 8581. (b) Sun, S.; Murray, C. B.; Doyle H. *Mater. Res. Soc. Symp. Proc.* **1999**, *577*, 385. (c) Sun, S.; Murray, C. B. *J. Appl. Phys.* **1999**, *85*, 4325. (d) Murray, C. B.; Sun, S.; Doyle, H.; Betley, T. *MRS Bull.* **2001**, 985. (e) Cordente, N.; Respaud, M.; Senocq, F.; Casanove, M. J.; Amiens, C.; Chaudret, B. *Nano Lett.* **2001**, *1*, 565. (f) Dumestre, F.; Chaudret, B.; Amiens, C.; Respaud, M.; Fejes, P.; Renaud, P.; Zurcher, P. *Angew. Chem., Int. Ed.* **2003**, *42*, 5213. (g) Dumestre, F.; Chaudret, B.; Amiens, C.; Fromen, M.-C.; Casanove, M.-J.; Respaud, M.; Zurcher, P. *Angew. Chem., Int. Ed.* **2002**, *41*, 4286. (h) Puntes, V. F.; Krishan, K. M.; Alivisatos, A. P. *Science* **2001**, *291*, 2115. (i) Puntes, V. F.; Zanchet, D.; Erdonmez, C. K.; Alivisatos, A. P. *J. Am. Chem. Soc.* **2002**, *124*, 12874. (j) Shevchenko, E. V.; Talapin, D. V.; Rogach, A. L.; Kornowski, A.; Haase, M.; Weller, H. *J. Am. Chem. Soc.* **2002**, *124*, 11 480. (k) Shevchenko, E. V.; Talapin, D. V.; Schnablegger, H.; Kornowski, A.; Festin, Ö.; Svedlindh, P.; Haase, M.; Weller, H. *J. Am. Chem. Soc.* **2003**, *125*, 9090. (l) Govor, L. V.; Bauer, G. H.; Reiter, G.; Shevchenko, E.; Weller, H.; Parisi, J. *Langmuir* **2003**, *19*, 9573. (m) Suslick, K. S.; Fang, M.; Hyeon, T. *J. Am. Chem. Soc.* **1996**, *118*, 11960. (n) Farrell, D.; Majetich, S. A.; Wilcoxon, J. P. *J. Phys. Chem. B* **2003**, *107*, 11022. (o) Dumestre, F.; Chaudret, B.; Amiens, C.; Renaud, P.; Fejes, P. *Science* **2004**, *303*, 821.

(4) (a) Tang, Z. X.; Sorensen, C. M.; Klabunde, K. J.; Hadjipanayis, G. C. *J. Colloid Interface Sci.* **1991**, *146*, 38. (b) Chen, J. P.; Lee, K. M.; Sorensen, C. M.; Klabunde, K. J.; Hadjipanayis, G. C. *J. Appl. Phys.* **1994**, *75*, 5876. (c) Li, S.; John, V. T.; O'Connor, C.; Harris, V.; Carpenter, E. *J. Appl. Phys.* **2000**, *87*, 6223. (d) Feltin, N.; Pileni, M. P. *Langmuir* **1997**, *13*, 3927. (e) Fried, T.; Shemer, G.; Markovich, G. *Adv. Mater.* **2001**, *13*, 1158. (f) Moumen, N.; Pileni, M. P. *Chem. Mater.* **1996**, *8*, 1128. (g) Ngo, A. T.; Pileni, M. P. *Adv. Mater.* **2000**, *12*, 276. (h) Liu, C.; Zou, B.; Rondinone, A. J.; Zhang, Z. J. *J. Am. Chem. Soc.* **2000**, *122*, 6263. (i) Rondinone, A. J.; Samia, A. C. S.; Zhang, Z. J. *J. Phys. Chem. B* **2000**, *104*, 7919. (j) Rondinone, A. J.; Samia, A. C. S.; Zhang, Z. J. *J. Phys. Chem. B* **1999**, *103*, 6876. (k) Liu C.; Zou, B.; Rondinone, A. J.; Zhang, Z. J. *J. Phys. Chem. B* **2000**, *104*, 1141. (l) Kang, Y. S.; Risbud, S.; Rabolt, J. F.; Stroeve, P. *Chem. Mater.* **1996**, *8*, 2209. (m) Chen, J. P.; Sorensen, C. M.; Klabunde, K. J.; Hadjipanayis, G. C.; Devlin, E.; Kostikas, A. *Phys. Rev. B* **1996**, *54*, 9288. (n) Zhang, Z. J.; Wang, Z. L.; Chakoumakos, B. C.; Yin, J. S. *J. Am. Chem. Soc.* **1998**, *120*, 1800. (o) Hong, C.-Y.; Jang, I. J.; Horng, H. E.; Hsu, C. J.; Yao, Y. D.; Yang, H. C. *J. Appl. Phys.* **1997**, *81*, 4275. (p) Carpenter, E. E.; O'Connor, C. J. *J. Appl. Phys.* **1999**, *85*, 5175. (q) Vestal, C. R.; Zhang, Z. J. *J. Am. Chem. Soc.* **2003**, *125*, 9828.

(5) (a) Easom, K. A.; Klabunde, K. J.; Sorensen, C. M. *Polyhedron* **1994**, *13*, 1197. (b) Rockenberger, J.; Scher, E. C.; Alivisatos, A. P. *J. Am. Chem. Soc.* **1999**, *121*, 11595. (c) Shafi, K. V. P. M.; Gedanken, A. *Chem. Mater.* **1998**, *10*, 3445. (d) Guo, Q.; Teng, X.; Rahman, S.; Yang, H. *J. Am. Chem. Soc.* **2003**, *125*, 630.

(6) (a) Hyeon, T.; Lee, S. S.; Park, J.; Chung, Y.; Na, H. B. *J. Am. Chem. Soc.* **2001**, *123*, 12798. (b) Hyeon, T.; Chung, Y.; Park, J.; Lee, S. S.; Kim, Y.-W.; Park, B. H. *J. Phys. Chem. B* **2002**, *106*, 6831.

(7) (a) Sun, S.; Zeng, H. *J. Am. Chem. Soc.* **2002**, *124*, 8204. (b) Sun, S.; Zeng, H.; Robinson, D. B.; Raoux, S.; Rice, P. M.; Wang, S. X.; Li, G. *J. Am. Chem. Soc.* **2004**, *126*, 273.

(8) (a) Joo, J.; Na, H. B.; Yu, T.; Yu, J. H.; Kim, Y. W.; Wu, F.; Zhang, J. Z.; Hyeon, T. *J. Am. Chem. Soc.* **2003**, *125*, 11100. (b) Joo, J.; Yu, T.; Kim, Y. W.; Park, H. M.; Wu, F.; Zhang, J. Z.; Hyeon, T. *J. Am. Chem. Soc.* **2003**, *125*, 6553. (c) Kim, S.-W.; Park, J.; Jang, Y.; Chung, Y.; Hwang, S.; Kim, Y. W.; Hyeon, T. *Nano Lett.* **2003**, *3*, 1289.

(9) Brabers, V. A. M. *Handbook of Magnetic Materials*; Buschow, K. H. J., Ed.; North-Holland: Amsterdam, 1995.

(10) Liu, C.; Zhang, Z. J. *Chem. Mater.* **2001**, *13*, 2092.